

# CONESCAPANHONDURAS2025paper142.pdf

 Institute of Electrical and Electronics Engineers (IEEE)

---

## Document Details

### Submission ID

trn:oid:::14348:477735194

### Submission Date

Jul 31, 2025, 9:52 PM CST

### Download Date

Aug 12, 2025, 6:32 PM CST

### File Name

CONESCAPANHONDURAS2025paper142.pdf

### File Size

324.3 KB

6 Pages





4,966 Words

25,797 Characters




# 19% Overall Similarity

The combined total of all matches, including overlapping sources, for each database.

## Match Groups

-  **42 Not Cited or Quoted 16%**  
Matches with neither in-text citation nor quotation marks
-  **8 Missing Quotations 2%**  
Matches that are still very similar to source material
-  **4 Missing Citation 2%**  
Matches that have quotation marks, but no in-text citation
-  **0 Cited and Quoted 0%**  
Matches with in-text citation present, but no quotation marks

## Top Sources

- 14%  Internet sources
- 18%  Publications
- 0%  Submitted works (Student Papers)

## Integrity Flags





### 0 Integrity Flags for Review

No suspicious text manipulations found.




Our system's algorithms look deeply at a document for any inconsistencies that would set it apart from a normal submission. If we notice something strange, we flag it for you to review.

A Flag is not necessarily an indicator of a problem. However, we'd recommend you focus your attention there for further review.

## Match Groups

-  **42 Not Cited or Quoted 16%**  
Matches with neither in-text citation nor quotation marks
-  **8 Missing Quotations 2%**  
Matches that are still very similar to source material
-  **4 Missing Citation 2%**  
Matches that have quotation marks, but no in-text citation
-  **0 Cited and Quoted 0%**  
Matches with in-text citation present, but no quotation marks

## Top Sources

- 14%  Internet sources
- 18%  Publications
- 0%  Submitted works (Student Papers)

## Top Sources

The sources with the highest number of matches within the submission. Overlapping sources will not be displayed.

1	Publication	Yuan Zhang, Yupeng Yang, Shuai Lu, Enwen Zhou. "Development and Outlook for...	1%
2	Internet	v.vibdoc.com	1%
3	Publication	Nijia Ye, Bo Hu. " Kinematic and Stiffness Modeling of a Novel 3-DOF + + Parallel ...	1%
4	Internet	ddd.uab.cat	<1%
5	Publication	Jibril A. Bala, Steve A. Adeshina, Abiodun M. Aibinu. "Implementing Nonlinear Mo...	<1%
6	Publication	Qixian Wang, Qinghua Meng, Lidan Chen, Haibin He. "Homogeneous Domination...	<1%
7	Internet	ris.utwente.nl	<1%
8	Publication	Martín Medina-Sánchez, Alejandro G. Yepes, Óscar López, Ayman Samy Abdel-Kha...	<1%
9	Publication	Alexandr Stefek, Van Thuan Pham, Vaclav Krivanek, Khac Lam Pham. "Energy Co...	<1%
10	Internet	www.drroyspencer.com	<1%

11	Internet	arxiv.org	<1%
12	Publication	Junbin Liang, Haihan Zhang, Xia Deng, Zongjian He. "On Zone-Differentiated Time...	<1%
13	Publication	Said Fadlo, Abdelhafid Ait Elmahjoub, Nabila Rabbah. "Energy Performance Analy...	<1%
14	Internet	riuma.uma.es	<1%
15	Internet	scholar.sun.ac.za	<1%
16	Publication	Haidong Zhang, Zhichao Meng, Zhenggang Guo, Xiaoqi Huang, Junzhou Huo. "Mo...	<1%
17	Internet	ijeecs.iaescore.com	<1%
18	Publication	Huihui Sun, Yujie Zhang, Bin Xie, Bin Zi. "Dynamic modeling and error analysis of ...	<1%
19	Publication	Shoulu Gong, Jiahao Wu, Tianxiang Zheng, Wen-Ming Zhang, Lei Shao. "Untether...	<1%
20	Internet	www.science.org	<1%
21	Internet	www.hindawi.com	<1%
22	Publication	Luqi Tang, Fuwu Yan, Bin Zou, Kewei Wang, Chen Lv. "An Improved Kinematic Mo...	<1%
23	Publication	Cho W. S. To. "Engineering Dynamics", Springer Science and Business Media LLC, ...	<1%
24	Internet	robotics.itee.uq.edu.au	<1%

25	Publication	Shuwei Pang, Qiuhong Li, Hailong Feng, Haibo Zhang. "Joint Steady State and Tra...	<1%
26	Internet	epdf.tips	<1%
27	Publication	Chao Chen, Wesley Au, Shao Liu. "Robotics - From Theory to Practice", CRC Press, ...	<1%
28	Publication	Shaotong Pei, Haichao Sun, Weiqi Wang, Bing Xiao, Hengjiang Zhu, Mianxiao Wu, ...	<1%
29	Publication	Ibrahim A. Seleem, Haitham El-Hussieny, Hiroyuki Ishii. "Imitation-Based Motion ...	<1%
30	Publication	Miguel O. Arias Estrada, Alejandro Espinosa Manzo, Monica Wendoly Cruz Ramire...	<1%
31	Internet	es.scribd.com	<1%
32	Internet	seal.matrade.gov.my	<1%
33	Publication	Morales, J., J.L. Martinez, A. Mandow, A.J. Garcia-Cerezo, and S. Pedraza. "Power C...	<1%
34	Publication	Ximena Toalongo, César Trelles, Ángel Alsina. "Design, Construction and Validatio...	<1%
35	Internet	www.mdpi.com	<1%
36	Publication	"AETA 2022—Recent Advances in Electrical Engineering and Related Sciences: The...	<1%
37	Internet	digital.library.unt.edu	<1%
38	Publication	Fraser, B.J.. "Syntheses of educational productivity research", International Journ...	<1%

# Development of a kinematic model based on simulation data for a three symmetrical wheeled pipeline robot

XXXXXX XXXXX XXXXX  
XXXXXXXXXX  
XXXXXXXXXX  
XXXXXXXXXX  
XXXXXX

XXXX XXXX XXXX  
XXXXXXXXXX  
XXXXXXXXXX  
XXXXXXXXXX  
XXXXXX

XXXX XXXX XXXX  
XXXXXXXXXX  
XXXXXXXXXX  
XXXXXXXXXX  
XXXXXX

XXXX XXXX XXXX  
XXXXXXXXXX  
XXXXXXXXXX  
XXXXXXXXXX  
XXXXXX

**Abstract**—This study presents the development, modeling, and validation of a type 3-RRR planar parallel manipulator, with the primary objective of solving the direct kinematics problem using artificial neural networks. The robot's design was carried out in SolidWorks, where circular trajectories were simulated to collect training data. Later, a feedforward neural network was trained in a Python development environment (Spyder), using joint coordinates as inputs and Cartesian positions as outputs. The network was validated with error metrics that demonstrate high accuracy in predicting the position of the end effector. The results confirm that this artificial intelligence-based approach offers an efficient, precise, and computationally inexpensive alternative for the kinematic modeling of parallel robots, being applicable to real-time systems and industrial environments that require high repeatability.

**Index Terms**—Keywords: Planar Robot, SolidWorks, 3RRR, Robotics, Deep Learning

## I. INTRODUCTION

Robots for internal inspection of pipelines have had a great growth in the analysis for the search of leaks, but according to the internal route of the pipeline, several difficulties may arise. Mainly in the T-shaped routes and with several elbows, is where the displacement of the robot is complicated making necessary more joints at the expense of a slower speed at the moment of moving [1] [2]. As autonomous robots move internally through the pipelines, the kinematic models together with the autonomy they possess offer greater precision for the result of the positions or interactions with the environment [3]. Creating a relationship gap between the kinematic models of the robots together with Deep learning for the parameter setting of output and input variables according to the situation. The design of robots for pipelines is oriented to whether the route is internal or external to the pipeline, generating a lack of integration between both models of interaction with the environment where the longest routes are in the pipelines pass underground by high distributions as in the oil and water sector [4]. A mobile robot for straight paths is responded with wheel

mechanisms according to the fast torque response together with the control of the flexibility of the movement where the wheels of the robot itself can move independently of the environment [5]. Offering a faster and more responsive option to the need for long-distance pipeline safety.

## II. MATERIALS AND METHODS

### A. Mathematical Model

For mobile robots that are autonomous and travel long distances, initial tracking controllers are primarily built using the geometric model of the vehicle and feedback control theory. This is due to the simplicity and stability they offer; that is, the deflection inputs of the feedback controller are derived from the geometric relationship between the vehicle and the road [1]. Mathematical modeling for analysis in different axes or phases of the movement, there are techniques such as vector space decomposition (VSD) for matrix visualization and graphing [3]. Mathematical models have a correlation in mobile robot controllers along with their analysis techniques as vector space [6]. Designing a control algorithm for continuous manipulators or mobile robots that can interact robustly in dynamic environments represents a significant challenge as they are nonlinear systems due to the parameters of each environment [7]. Using software such as Matlab and Simulink, control and resolution diagrams are applied to the mathematical models associated with robotics [8]. Another graphical way of visualization for mathematical models is by means of vertical flow diagrams similar to control charts where scaling methods only consider the adaptation of the performance of multiple discrete steady state discrete points, but ignore the adaptation of transient performance [9]. These main points are in accordance with the expected response of the mathematical model to the study being carried out.

1) *Environment Reference System*: The reference system describes the coordinate framework used to define the position and orientation of objects in a three-dimensional space. It consists of a set of Cartesian axes (x, y, z) used to describe the initial location of the robot. In the SolidWorks simulation environment, rectangular Cartesian coordinate system is used.

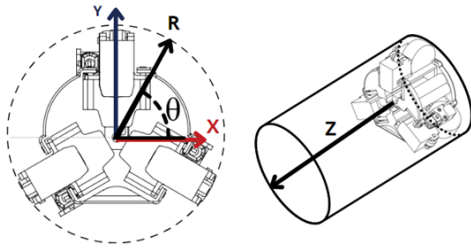


Fig. 1: Cylindrical coordinate system of the mobile robot

However, for the analysis of state variables considering the robot's applications and the geometry of the environment where it will be located, a cylindrical coordinate system was chosen. For the following reasons and conditions.

- Pipes typically have a cylindrical shape, so using cylindrical coordinates allows for a natural and precise description of the environment in which the robot operates.
- In the XY plane, it is more efficient to describe the radial distance, which would be the radius of the internal pipe where the robot is located, with respect to its own center of mass.
- Cylindrical coordinates simplify the description of the robot's position and orientation in relation to the longitudinal axis of the pipe, which facilitates programming and motion control.

2) *Kinematic Model*: Kinematics focuses on the analytical description of the robot's spatial motion as a function of time, especially on the relationships between the position and orientation of its endpoint with the values of the joint coordinates [10]. Currently, techniques for solving the direct and inverse kinematics of serial and parallel mechanisms mainly include the analytical method and the numerical optimization method. The analytical method involves the use of algebraic or geometric methods to directly solve the solution, generating multiple unitary equations by elimination [11]. For the study and the elaboration of a kinematic analysis according to a mobile robot that goes internally on surfaces that can be straight or with a certain degree of inclination and if it is driven with a differential traction. The kinematics of differential traction, when referring to the movement of a vehicle, is significantly influenced by various elements associated with the dynamics of the vehicle. Among these determining factors are the position of the center of gravity, the peculiarities of the terrain over which the vehicle travels and the inclination of the terrain in relation to the surface [12]. Along with the demand for irregularly shaped components has increased, the stiffness requirements of each direction are inconsistent during the processing of the traction generated by the robot itself [13]. Thus, the complex interaction between kinematics and dynamics is manifested through the dynamic interplay between the center of gravity, terrain characteristics and ground inclination, creating an environment where optimization and understanding of these factors is essential for effective and safe movement of the vehicle or mobile robot. Pipeline inspection

robots, whether wheel or snake type, which use the rotational force of an electric motor to drive them, tend to be bulky as they employ considerable forces when pulling endoscopes and cables, making them difficult to apply in narrow and long distance pipeline inspections. The notion of a pseudorigid body model in order to obtain a more accurate kinematic representation of compliant mechanisms [14]. Kinematic modeling can take advantage of the properties of its closed-loop configuration. The notion of a pseudorigid body model in order to obtain a more accurate kinematic representation of the conformal mechanisms [15]. Giving a wide range of benefits in the control of long trajectories on mobile robots. A crucial consideration in addressing the differential driving of mobile robots is that the design of their motion controller is mainly based on kinematic models. This is because dynamic models are more complex than kinematic models, and mobile robots generally use only the low motor speed to control loop [16]. According to [17] describes that a motion is considered translational when all straight lines within the body maintain a constant direction during that motion. On the other hand, in the case of rotation, the particles that compose the rigid body move in parallel planes along circles centered on a fixed axis called the axis of rotation. When this axis crosses the rigid body, the particles located on this axis have zero velocity and acceleration. When describing a rotational motion, the most appropriate measure for the angle  $\theta$  is in radians instead of degree where the coordinate  $\theta$  indicates the angular position of a rigid body at a specific time [18]. We can analyze the rotational motion of the rigid body by considering the rate of change of  $\theta$ , similar to how linear motion is described. Defining the rate of change of the angular coordinate as the average angular velocity of the system itself. If the angular velocity of a rigid body changes, angular acceleration occurs.

$$\alpha = \frac{d\omega}{dt} = \frac{d^2\theta}{dt^2} = \frac{\omega d\omega}{d\theta} \quad (1)$$

Where  $\omega$  is the angular velocity of the rigid body and is the angular acceleration. When a rigid object rotates around a stationary axis, all its particles follow a circular trajectory. This circumference is located in a plane that is perpendicular to the axis and has its center at the latter. The velocity of a particle is directly related to the angular velocity of the object; as the object rotates faster, the velocity of each particle increases. This refers to wheels rotating around a fixed axis, where each revolution results in a linear speed determined by this rotation.

$$v = \omega * r \quad (2)$$

Where  $r$  is the radius of the rigid body to be analyzed or generally the wheels associated with the mobility of mobile robots. While the analysis of the acceleration varies due to the circular motion. The accelerations in this type of systems can be classified into two types: tangential acceleration and radial acceleration [18].

$$a_{\text{tan}} = r * \alpha, a_{\text{rad}} = \omega^2 * r \quad (3)$$

3) *State Variables of the control system*: State variables are those that fully describe the state of a system at a given time [19]. They are usually represented in the form of matrices and are subdivided into two groups.

- **Input Variables or Control Variables**: These are the variables that are configurable or manipulable by the user.
- **Output Variables**: These are the variables that are the effect caused by the manipulation of the input variables.

$$u(t) = \begin{bmatrix} \omega_1 \\ \omega_2 \\ \omega_3 \end{bmatrix}, \quad y(t) = \begin{bmatrix} r \\ \theta \\ z \end{bmatrix}, \quad y'(t) = \begin{bmatrix} \dot{r} \\ \dot{\theta} \\ \dot{z} \end{bmatrix}, \quad (4)$$

Where each matrix with its set of variables is defined as:

- $u(t)$ : is the matrix of the control variables of the mobile robot. Each  $\omega$  represents the angular velocity that each of the motors has in revolutions per minute (rpm) values.
- $y(t)$ : It is the matrix of output variables in the kinematic model that represents the agreed reference system. We relate the Cartesian axes in cylindrical coordinates where  $r$  represents the radial distance in an XY plane with a physical magnitude in millimeters (mm),  $\theta$  represents the orientation or azimuthal angle in the XY plane with a physical magnitude in radians (rad), and  $z$  represents the linear displacement of the robot along the pipe with a physical magnitude in mm.
- $y'(t)$ : Is the matrix representing the rate of change of the initial variables of the output matrix. Where  $\dot{r}$  the radial velocity in physical magnitudes of millimeters per second (mm/s),  $\dot{\theta}$  represents the angular velocity of the robot around the z-axis in physical magnitudes of radians per second (rad/s) and  $\dot{z}$  is the linear velocity along the robot's path with a physical magnitude in mm/s.

### III. RESULTS

#### A. Design Analysis

#### B. Analysis of the mathematical model

Each simulation developed in Solidworks software was taken into account with a gravity of 9,806.65 millimeters per second squared in the Y-axis. The displacement of the robot was taken into account in the positive Z-axis. Each study was taken on a 5-second time basis to test different velocities along the same duct. It was also assumed that the wheels do not slip along the path. Each test was taken into account on the basis of the 3 motors out of phase at 120 degrees to each other. Named  $\omega_1$ ,  $\omega_2$  and  $\omega_3$  correspondingly for the simulation environment and data acquisition of each value.

1) *Kinematic Analysis*: In this section, we will define each variable related to the direct kinematics of the mobile robot along with its approach and the specific conditions that were taken into account when performing the studies and equations.

a) *Radial Distance and Radial Velocity*: The radial distance of the system represents the radius of the pipe where the robot is located in a cylindrical coordinate system. This

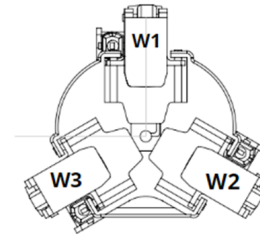


Fig. 2: Location of the reference variables to the motors

Fig. 3: Degree and time ratio of motors at 10 rpm

variable reflects the relationship of the Cartesian XY coordinates in a two-dimensional plane, taking them as a resultant in that plane. For this analysis the following conditions were taken into account:

- The R value being the radius of the pipe, it will be assumed that the pipe is ideal and remains constant during the entire path.
- The change of the radial distance is null since there is no variation in the geometry of the pipe along the path.

$$R = 7.98in = 202.72mm = constant, \quad \dot{R} = 0mm/s \quad (5)$$

b) *Angular Coordinate*: The angular coordinate describes the degree of inclination the robot has along the pipe path. Having only 3 input variables, which are the angular velocities corresponding to each of the motors, 3 types of situations for the robot were taken into account.

- When all angular velocities are 0
- When all angular velocities are the same and greater than 0.
- When one angular velocity is different with respect to the other.

In the first condition was obtained the initial degree which is the value that is outside the x-value. Where for the beginning a value in degrees of -0.2141 degrees was taken as the initial condition of the system. In the second condition, several samples were taken when turning off one of the motors to see the behavior of the robot. In the fig 3 it is taken with identical angular velocities of 10 rpm corresponding to the motors that are on. So, in a short period of time up to the time of 2 seconds, the system behaves in a constant way between the range of values from -0.15 to -0.2 degrees.

- Having the same angular velocities, it tends to the same initial conditions with slight changes with increasing angular velocity.
- The increase and decrease of the angular coordinate are dependent on the two corresponding motors  $\omega_2$  and  $\omega_3$

$$\theta = (-0.0013 \left( \frac{\omega_1 + \omega_2 + \omega_3}{3} \right)) (e^{-0.25t} + 1) \quad (6)$$



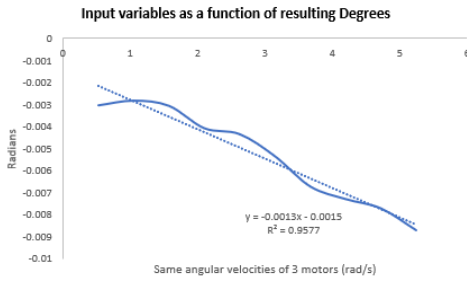


Fig. 4: Input Variables as a function of resulting degrees

In (7), the value obtained is in radians, therefore, at the time of comparison with the Solidworks results, a conversion to degrees per second was made. To obtain the constants that are described as a subtraction, the averages of the angular coordinates resulting from each of the tests were obtained. Where the slope of the linear regression represents the average of the 3 motors as one. The use of the Euler values was to describe the abrupt behavior that the robot has at the beginning when each of the motors is driven until it reaches the average value established by the first parenthesis with an attenuation of 0.25. Being this attenuation in the Euler value as the reciprocal of the time minus 1. This value can be further decreased, but it is only so that the trend of the value is increasing to the averaged value.

$$\theta = (-0.0013 \left( \frac{\omega_1 + \omega_2 + \omega_3}{3} \right)) (e^{-0.25t} + 1) + \frac{t}{80} \left( \frac{\omega_2 - \omega_3}{\omega_1 + \omega_2 + \omega_3 + 0.001} \right) \quad (7)$$

c) *Angular Velocity*: The angular velocity and the angular coordinate were compared in the same instances. In ideal cases, there should not be an angular velocity in each sample. The results in Solidworks showed an oscillatory behavior by having the same angular velocity with respect to each motor. The trend of the angular velocity values always lies at 0, but the higher the angular velocity that was imposed, the more oscillatory motion was generated, denoting the high vibrations of the mobile robot. The derivation of (8) was based on the conditions established as a definition of state variables in (4). Once the angular coordinate was obtained, its time derivative was computed to determine the corresponding angular velocity according to its physical definition.

As a result, the derivative of the angular coordinate will tend to 0, if the velocities are equal.

$$\dot{\theta} = (-0.0013 \left( \frac{\omega_1 + \omega_2 + \omega_3}{3} \right)) (-0.25e^{-0.25t}) + \frac{1}{80} \left( \frac{\omega_2 - \omega_3}{\omega_1 + \omega_2 + \omega_3 + 0.001} \right) \quad (8)$$

d) *Linear Displacement*: The linear displacement was oriented to the Z variable of the output variable matrix. In the Solidworks analysis it was taken into account from the center of mass of the robot. The behavior of this variable is simpler than with the rest. Because the robot can only move in one direction, which can be either forward or backward of the pipe itself. Therefore, the result showed a linear behavior

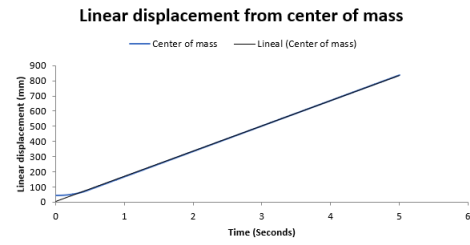


Fig. 5: Linear displacement from Center of mas

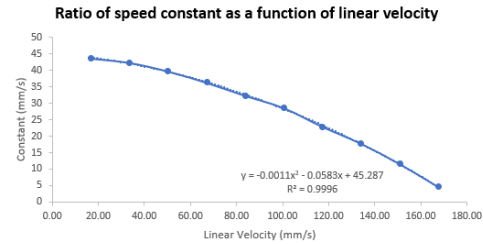


Fig. 6: Ratio of speed constant as a function of linear velocity

as shown in Fig. 6, which was one of the tests using angular velocities at 50 rpm in each of the engines. Despite the great turbulence in the angular velocities shown in the previous section, the displacement presents a behavior that is easy to interpret. Where another result was also obtained, which was the decrease of the constant formed at par of the tangent line as a function of the increase of the linear velocity. The slope of the linear regression denotes the derivative of the linear displacement formed which would be in any case the linear velocity in the direction of Z generated by the ratio of the angular velocities of the motors.

Figure 7 shows a quadratic function showing how the constant decreases as a function of increasing linear velocities. Where  $\dot{z}$  is the derivative of the linear displacement along the Z-axis of the robot along its path.

$$z = \dot{z} * t - 0.0011 * \dot{z}^2 - 0.0583 * \dot{z} + 45.287 \quad (9)$$

e) *Linear Velocity*: The linear velocity along the z-axis is dependent on the angular velocities of each of the motors. Where each angular velocity results in a linear speed in the same direction if activated for translation. In [16] their kinematic model for a mobile robot used the average of linear velocities to obtain a single resultant, but in a 2D plane. The same method was implemented in this study, considering that it only moves in one direction and the resultant goes in the same direction.

$$\dot{z} = r * \left( \frac{\pi}{30} \right) * \left( \frac{\omega_1 + \omega_2 + \omega_3}{3} \right) \quad (10)$$

The reason for the value of  $\pi/30$  is for the conversion from rpm to radians per second, and the radius used corresponds to the geometry of the wheels. Wheels with a diameter of 32 mm were used as a characteristic value of the robot system.

Assuming the system as a singular average generates a specific value when all angular velocities are equal. However, upon variation of one of them, a slight change is observed,

as depicted in Fig. 8 when comparing the results to a single motor with higher angular velocity.

$$\dot{z} = r \left( \frac{\pi}{30} \right) \left( \frac{\omega_1 + \omega_2 + \omega_3}{3} + \frac{1230}{2737} \sqrt{(\omega_1 - \omega_2)^2 + (\omega_1 - \omega_3)^2 + (\omega_2 - \omega_3)^2} \right)$$

In (12), the correction factor is the result of the squared sums of the differences in angular velocities with respect to each motor. This serves as a method to compensate for the average velocity when their values are significantly different from one another. The constant multiplying the resultant of the deviations is a value representing the deviation ratio between the expected value, projected in Solidworks, and the resulting value obtained from the average of angular velocities with differing values.

$$FC = \frac{v_{\text{solid}} - v_{\text{calc}}}{\sqrt{(\omega_1 - \omega_2)^2 + (\omega_1 - \omega_3)^2 + (\omega_2 - \omega_3)^2}} \approx \frac{1230}{2737} \quad (11)$$

2) *Comparative Tests:* To perform a comparison of the results obtained in SolidWorks with respect to the equations, a simulation environment was designed and configured in Simulink. This environment was meticulously structured to allow the evaluation and testing of the equations of both models. A link was established between the models created in SolidWorks and Simulink, using the spreadsheet exported from SolidWorks as a connecting bridge. This spreadsheet not only facilitated the transfer of data between the two environments, but also provided a platform to graphically visualize the behavior of the systems and the final results. The comparison process was carried out with a rigorous analysis of the data generated during a simulation time of 5 seconds. This period was considered sufficient to obtain a complete perspective of the behavior of the model in both environments. Table I shows a comparison between the results obtained through simulations and those generated by the proposed model.

During this evaluation phase, the discrepancies and similarities between the results obtained in SolidWorks and those derived from the equations implemented in Simulink were examined in detail. With a total of 6 final samples to compare the performance, the accuracy and deviation of the mathematical model were compared. Table II presents the results of a paired samples t-test comparing the proposed matlab model (Mat\_MD) with the SolidWorks Simulation (Solid\_Sim) under two loading conditions: vertical load (LV) and diagonal load (LD). In both cases, the p-values are greater than 0.05, indicating no statistically significant difference between the two methods. Having a maximum accuracy of 98.94 % for the kinematic model. These results suggest that the proposed model yields results comparable to those obtained from SolidWorks, supporting its validity for structural simulation in these scenarios.

#### IV. DISCUSSION

The proposed kinematic and dynamic model for the three-wheeled robot demonstrates suitable capabilities for navigating confined environments such as industrial pipelines, meeting the mobility, stability, and precision requirements needed for inspection tasks comparing it with the basis of [20] and [21]. Unlike previous studies that focus on tracked or articulated robots like [9], our approach based on a differential tricycle configuration reduces mechanical complexity and energy consumption, allowing a lighter and more flexible implementation. Compared to the four-wheeled model presented by [5] and [22], our design offers advantages when navigating tight curves or narrow sections, due to its smaller turning radius and compact overall size. However, it also presents limitations in traction on slippery surfaces [23], a challenge partially addressed by dynamically adjusting the speed based on the detected friction. Regarding the dynamic model, contact forces with the inner walls of the pipe were integrated, an aspect not considered in studies such as [7], which focused on flat surface motion. This enhancement enabled a more realistic simulation of the robot's behavior under actual pipe conditions, including inclinations and variations in diameter like in [14]. One identified limitation in our model is the simplification of the wheel-surface contact as a point interaction, without considering structural deformations, which may introduce minor errors in irregular environments like [1] and [24]. Future work may incorporate more complex contact models or simulations in pipelines with variable surface roughness. Overall, the results validate the proposed model as a solid foundation for autonomous robot control, with promising prospects for integrating real-time sensors and intelligent navigation in industrial and urban pipeline networks. As shown in Figure 11, the comparison between the results obtained from the equations simulated in MATLAB and those derived from SolidWorks reveals a close agreement. The discrepancies observed between both methods are minimal, indicating a small margin of error in the evaluated variables.

#### V. CONCLUSIONS

This research successfully developed and validated kinematic models for a three-wheeled mobile robot intended for pipe inspection. By integrating SolidWorks for mechanical design and MATLAB Simulink for simulation, the study provided a detailed understanding of the motion of the robot and the forces acting on it. The kinematic model demonstrated high accuracy (96.28%) in predicting positional behavior, effectively capturing the system's response to motor inputs

TABLE I: Comparison of results between SolidWorks Simulation and the proposed model for linear velocity (LV) and linear displacement (LD) under various angular velocities.

Angular Velocity (rad/s)	SolidWorks LV	Proposed LV	SolidWorks LD	Proposed LD
5,5,5	16.7	16.8	128.9	127.9
3,5,7	23.5	24.1	159.5	164.0
10,10,10	33.5	33.5	212.4	209.8
15,15,15	50.3	50.3	295.5	291.0
20,20,20	67.0	67.0	379.4	371.7
25,25,25	83.7	83.8	462.7	451.7

TABLE II: Resultados de la prueba de muestras emparejadas entre el modelo propuesto (Mat\_MD) y SolidWorks Simulation (Solid\_Sim).

Par	Media	Desv.	Desv. Error	IC 95% Inf.	IC 95% Sup.	t	gl	Sig. (bilateral)
Solid_Sim_LV - Mat_MD_LV	-0.13333	0.23381	0.09545	-0.37870	0.11203	-1.397	5	0.221
Solid_Sim_LD - Mat_MD_LD	3.71667	5.39756	2.20355	-1.94773	9.38106	1.687	5	0.152

and torque demands. The analysis highlighted the model's sensitivity to motor speed variations, revealing a reduction in predictive precision at higher speeds, an important consideration for real-world applications. Limiting the mathematical model for implementation at low rpm speeds, due to its imbalance. Despite this, the model maintained robust performance, which makes it suitable for the development and optimization of control systems in pipe inspection tasks. In general, the findings provide a solid foundation for the implementation of autonomous navigation and real-time control in confined environments. Future work may focus on incorporating adaptive control algorithms and real-time sensor feedback to further enhance model accuracy and robot performance under dynamic operational conditions.

## REFERENCES

- [1] L. Tang, F. Yan, B. Zou, K. Wang, and C. Lv, "An improved kinematic model predictive control for high-speed path tracking of autonomous vehicles," *IEEE Access*, vol. 8, pp. 51 400–51 413, 2020.
- [2] S. Kazeminasab and M. K. Banks, "A localization and navigation method for an in-pipe robot in water distribution system through wireless control towards long-distance inspection," *IEEE Access*, vol. 9, pp. 117 496–117 511, 2021.
- [3] A. M. Shata, A. S. Abdel-Khalik, R. A. Hamdy, M. Z. Mostafa, and S. Ahmed, "Improved mathematical modeling of six phase induction machines based on fractional calculus," *IEEE Access*, vol. 9, pp. 53 146–53 155, 2021.
- [4] D. Xie, J. Liu, R. Kang, and S. Zuo, "Fully 3d-printed modular pipe-climbing robot," *IEEE Robotics and Automation Letters*, vol. 6, no. 2, pp. 462–469, 2021.
- [5] H. Wang, C. Hu, W. Cui, and H. Du, "Multi-objective comprehensive control of trajectory tracking for four-in-wheel-motor drive electric vehicle with differential steering," *IEEE Access*, vol. 9, pp. 62 137–62 154, 2021.
- [6] T. Phuong Nguyen, H. Nguyen, N. Minh Ngo, and H. Q. T. Ngo, "Experimental verification of the field robotic system for pipeline maintenance," *IEEE Access*, vol. 13, pp. 13 782–13 795, 2025.
- [7] I. A. Seleem, H. El-Hussieny, and H. Ishii, "Imitation-based motion planning and control of a multi-section continuum robot interacting with the environment," *IEEE Robotics and Automation Letters*, vol. 8, no. 3, pp. 1351–1358, 2023.
- [8] M. Schluter and E. Perondi, "Mathematical modeling with friction of a scara robot driven by pneumatic semi-rotary actuators," *IEEE Latin America Transactions*, vol. 18, no. 06, pp. 1066–1076, 2020.
- [9] S. Pang, Q. Li, H. Feng, and H. Zhang, "Joint steady state and transient performance adaptation for aero engine mathematical model," *IEEE Access*, vol. 7, pp. 36 772–36 787, 2019.
- [10] A. Barrientos, *Fundamentos de robótica*. Madrid, Spain: McGraw-Hill España, 2012.
- [11] H. Sun, Y. Zhang, B. Xie, and B. Zi, "Dynamic modeling and error analysis of a cable-linkage serial-parallel palletizing robot," *IEEE Access*, vol. 9, pp. 2188–2200, 2021.
- [12] J. L. Martínez, J. Morales, J. M. García, and A. García-Cerezo, "Analysis of tread icrs for wheeled skid-steer vehicles on inclined terrain," *IEEE Access*, vol. 11, pp. 547–555, 2023.
- [13] N. Ye and B. Hu, "Kinematic and stiffness modeling of a novel 3-dof rpu+upu+spu parallel manipulator," *IEEE Access*, vol. 10, pp. 6304–6318, 2022.
- [14] X. Hu, F. Li, and G. Tang, "Kinematics analysis of 3 upup coupling parallel platform in the marine environment," *IEEE Access*, vol. 8, pp. 158 142–158 151, 2020.
- [15] F. Hou, M. Luo, and Z. Zhang, "An inverse kinematic analysis modeling on a 6-pss compliant parallel platform for optoelectronic packaging," *CES Transactions on Electrical Machines and Systems*, vol. 3, no. 1, pp. 81–87, 2019.
- [16] A. Stefek, T. V. Pham, V. Krivanek, and K. L. Pham, "Energy comparison of controllers used for a differential drive wheeled mobile robot," *IEEE Access*, vol. 8, pp. 170 915–170 927, 2020.
- [17] R. Hibbeler, *Ingeniería mecánica - Dinámica. 7ma Edición*. México: Prentice-Hall Hispanoamericana S.A., 1996.
- [18] S. Alrasheed, *Principles of Mechanics Fundamental University Physics*. Cham: Springer International Publishing, 2019.
- [19] K. Ogata, *Ingeniería de Control Moderna*. Madrid, Spain: Pearson Educación, 2010.
- [20] J. Till, V. Aloí, K. E. Riojas, P. L. Anderson, R. J. Webster III, and C. Rucker, "A dynamic model for concentric tube robots," *IEEE Transactions on Robotics*, vol. 36, no. 6, pp. 1704–1718, 2020.
- [21] S. Kazeminasab, N. Sadeghi, V. Janfaza, M. Razavi, S. Ziyadidegan, and M. K. Banks, "Localization, mapping, navigation, and inspection methods in in-pipe robots: A review," *IEEE Access*, vol. 9, pp. 162 035–162 058, 2021.
- [22] H. Yan, L. Wang, P. Li, Z. Wang, X. Yang, and X. Hou, "Research on passing ability and climbing performance of pipeline plugging robots in curved pipelines," *IEEE Access*, vol. 8, pp. 173 666–173 680, 2020.
- [23] M. Gao, M. Huang, K. Tang, X. Lang, and J. Gao, "Design, analysis, and control of a multilink magnetic wheeled pipeline robot," *IEEE Access*, vol. 10, pp. 67 168–67 180, 2022.
- [24] D. Zholtayev, D. Dauletiya, A. Tilekulova, D. Akimbay, M. Nursultan, Y. Bushanov, A. Kuzdeuov, and A. Yeshmukhametov, "Smart pipe inspection robot with in-chassis motor actuation design and integrated ai-powered defect detection system," *IEEE Access*, vol. 12, pp. 119 520–119 534, 2024.